2008 American Control Conference
Westin Seattle Hotel, Seattle, Washington, USA
June 11-13, 2008

Energy-Based Hybrid Control for the RTAC System: Experimental Results

Jevon M. Avis, Sergey G. Nersesov, Rungun Nathan

Abstract— **The concept of an energy-based hybrid controller involves a hybrid controller that emulates an approximately lossless hybrid dynamical system and exploits the feature that the states of the dynamic controller may be reset to enhance the overall energy dissipation in the closed-loop system. Specifically, the controller accumulates the emulated energy and when the states of the controller coincide with a high emulated energy level, then we can reset these states to remove the emulated energy so that the emulated energy is not returned to the plant. In this paper, we present a general framework for such energy-based hybrid control for lossless systems and implement it in real time on the rotational/translational proof-mass actuator (RTAC) system. The obtained experimental results agree with the theory and show the efficacy of the presented theoretical framework.**

I. Introduction

Energy-based control for Euler-Lagrange dynamical systems and Hamiltonian dynamical systems based on passivity notions has received considerable attention in the literature [1], [2], [3], [4], [5], [6]. This controller design technique achieves system stabilization by shaping the energy of the closed-loop system which involves the physical system energy and the controller emulated energy. Specifically, *energy shaping* is achieved by modifying the system potential energy in such a way so that the shaped potential energy function for the closed-loop system possesses a unique global minimum at a desired equilibrium point. Next, damping is *injected* via feedback control modifying the system dissipation to guarantee asymptotic stability of the closed-loop system. A central feature of this energy-based stabilization approach is that the Lagrangian system form is preserved at the closed-loop system level. Furthermore, the control action has a clear physical energy interpretation, wherein the total energy of the closed-loop Euler-Lagrange system corresponds to the difference between the physical system energy and the emulated energy supplied by the controller. Furthermore, a passivity-based control framework for port-controlled Hamiltonian systems is established in [7], [8], [9], [10], [11]. Specifically, the authors in [7], [8], [9] develop a controller design methodology that achieves stabilization via system passivation.

More recently, a novel energy-dissipating hybrid control framework for Lagrangian, port-controlled Hamiltonian, and dissipative dynamical systems has been developed in [12]. These dynamical systems cover a very broad spectrum of applications including mechanical, electrical, electromechanical, structural, biological, and power systems. The concept of an energy-based hybrid controller can be viewed as a feedback control technique that exploits the coupling between a physical dynamical system and an energy-based controller to efficiently remove energy from the physical system. Specifically, if a dissipative or lossless plant is at high energy level, and a lossless feedback controller at a low energy level is attached to it, then energy will generally tend to flow from the plant into the controller, decreasing the plant energy and increasing the controller energy [13]. Of course, emulated energy, and not physical energy, is accumulated by the controller. Conversely, if the attached controller is at a high energy level and a plant is at a low energy level, then energy can flow from the controller to the plant, since a controller can generate real, physical energy to effect the required energy flow. Hence, if and when the controller states coincide with a high emulated energy level, then we can *reset* these states to remove the emulated energy so that the emulated energy is not returned to the plant. In this case, the overall closed-loop system consisting of the plant and the controller possesses discontinuous flows since it combines logical switchings with continuous dynamics, leading to impulsive differential equations [14], [15], [16], [17]. Within the context of vibration control using resetting virtual absorbers, these ideas were first explored in [18].

In this paper, on the example of the RTAC system, we implement in real time a general framework for the energy-based hybrid control design for lossless dynamical systems developed in [12]. The RTAC system represents a translational oscillator and an attached to it rotational proof-mass. The nonlinear coupling between the rotational motion of the proof-mass and translational motion of the cart provide the basis for control. The problem of control design for the RTAC system received considerable attention in the literature. Stabilization of the RTAC system as a benchmark problem for nonlinear control design has been studied in [19], [20]. Design of backstepping and passive nonlinear controllers for the RTAC system appears in [19], [21], while [18] studies resetting virtual absorbers as a means for energy dissipation. In addition, parameter dependent switching controllers for the RTAC system were developed in [22]. In the current paper, the energy-based hybrid control framework is presented for lossless dynamical systems. However, it was shown in [17] that the same control framework is applicable in the case of dissipative dynamical systems. The experimental results obtained for the RTAC system are in agreement with numerical simulations.

II. Hybrid Control Design for Lossless Dynamical Systems

In this and the next section, we present an energy-based hybrid control framework for lossless and Euler-Lagrange systems. Specifically, we consider nonlinear dynamical systems $\mathcal{G}_{\rm p}$ of the form

$$\dot{x}_{\rm p}(t) = f_{\rm p}(x_{\rm p}(t),u(t)), \quad x_{\rm p}(0)=x_{\rm p0}, \quad t\geq 0, \tag{1}$$

$$y(t) = h_{\rm p}(x_{\rm p}(t)), \tag{2}$$

where $t\geq 0$, $x_{\rm p}(t)\in\mathcal{D}_{\rm p}\subseteq\mathbb{R}^{n_{\rm p}}$, $\mathcal{D}_{\rm p}$ is an open set with $0\in\mathcal{D}_{\rm p}$, $u(t)\in\mathbb{R}^m$, $y(t)\in\mathbb{R}^l$, $f_{\rm p}:\mathcal{D}_{\rm p}\times\mathbb{R}^m\rightarrow\mathbb{R}^{n_{\rm p}}$ is smooth

This research was supported in part by the Office of Research and Sponsored Projects at Villanova University.

J.M. Avis and S.G. Nersesov are with the Department of Mechanical Engineering, Villanova University, Villanova, PA 19085-1681, USA (jevon.m.avis@villanova.edu; sergey.nersesov@villanova.edu).

R. Nathan is with the Division of Engineering, Pennsylvania State University, Reading, PA 19610, USA (rungun.nathan@psu.edu).

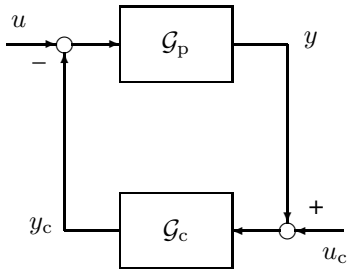

Fig. 1. Feedback interconnection of $\mathcal{G}_{\rm p}$ and $\mathcal{G}_{\rm c}$.

on $\mathcal{D}_{\rm p} \times \mathbb{R}^m$ and satisfies $f_{\rm p}(0,0) = 0$, and $h_{\rm p} : \mathcal{D}_{\rm p} \to \mathbb{R}^l$ is continuous and satisfies $h_{\rm p}(0) = 0$. Furthermore, for the nonlinear dynamical system $\mathcal{G}_{\rm p}$ we assume that the required properties for the existence and uniqueness of solutions are satisfied, that is, $u(\cdot)$ satisfies sufficient regularity conditions such that (1) has a unique solution forward in time.

Next, we consider hybrid resetting dynamic controllers $\mathcal{G}_{\rm c}$ of the form

$$\begin{aligned} \dot{x}_{\rm c}(t) &= f_{\rm cc}(x_{\rm c}(t), y(t)), \quad x_{\rm c}(0) = x_{\rm c0}, \\ &\qquad (x_{\rm c}(t), y(t)) \notin \mathcal{Z}_{\rm c}, \quad (3) \\ \Delta x_{\rm c}(t) &= \eta(y(t)) - x_{\rm c}(t), \quad (x_{\rm c}(t), y(t)) \in \mathcal{Z}_{\rm c}, \quad (4) \\ y_{\rm c}(t) &= h_{\rm cc}(x_{\rm c}(t), y(t)), \quad (5) \end{aligned}$$

where $x_{\rm c}(t) \in \mathcal{D}_{\rm c} \subseteq \mathbb{R}^{n_{\rm c}}$, $\mathcal{D}_{\rm c}$ is an open set with $0 \in \mathcal{D}_{\rm c}$, $y(t) \in \mathbb{R}^l$, $y_{\rm c}(t) \in \mathbb{R}^m$, $f_{\rm cc} : \mathcal{D}_{\rm c} \times \mathbb{R}^l \to \mathbb{R}^{n_{\rm c}}$ is smooth on $\mathcal{D}_{\rm c} \times \mathbb{R}^l$ and satisfies $f_{\rm cc}(0,0) = 0$, $\eta : \mathbb{R}^l \to \mathcal{D}_{\rm c}$ is continuous and satisfies $\eta(0) = 0$, and $h_{\rm cc} : \mathcal{D}_{\rm c} \times \mathbb{R}^l \to \mathbb{R}^m$ is continuous and satisfies $h_{\rm cc}(0,0) = 0$.

Recall that for the dynamical system $\mathcal{G}_{\rm p}$ given by (1) and (2), a function $s(u,y)$, where $s : \mathbb{R}^m \times \mathbb{R}^l \to \mathbb{R}$ is such that $s(0,0) = 0$, is called a *supply rate* [23] if it is locally integrable for all input-output pairs satisfying (1) and (2), that is, for all input-output pairs $u(\cdot) \in \mathcal{U}$ and $y(\cdot) \in \mathcal{Y}$ satisfying (1) and (2), $s(\cdot,\cdot)$ satisfies $\int_t^{\hat{t}} |s(u(\sigma), y(\sigma))| {\rm d}\sigma < \infty$, $t, \hat{t} \geq 0$. Here, $\mathcal{U}$ and $\mathcal{Y}$ are input and output spaces, respectively, that are assumed to be closed under the shift operator. Furthermore, we assume that $\mathcal{G}_{\rm p}$ is *lossless with respect to the supply rate* $s(u,y)$, and hence, there exists a continuous, nonnegative-definite *storage function* $V_{\rm s} : \mathcal{D}_{\rm p} \to \overline{\mathbb{R}}_+$ such that $V_{\rm s}(0) = 0$ and

$$V_{\rm s}(x_{\rm p}(t)) = V_{\rm s}(x_{\rm p}(t_0)) + \int_{t_0}^{t} s(u(\sigma), y(\sigma)) {\rm d}\sigma, \quad t \geq t_0,$$

for all $t_0, t \geq 0$, where $x_{\rm p}(t)$, $t \geq t_0$, is the solution to (1) with $u \in \mathcal{U}$. In addition, we assume that the nonlinear dynamical system $\mathcal{G}_{\rm p}$ is *completely reachable* [23] and *zero-state observable* [23], and there exists a function $\kappa : \mathbb{R}^l \to \mathbb{R}^m$ such that $\kappa(0) = 0$ and $s(\kappa(y), y) < 0$, $y \neq 0$, so that all storage functions $V_{\rm s}(x_{\rm p})$, $x_{\rm p} \in \mathcal{D}_{\rm p}$, of $\mathcal{G}_{\rm p}$ are positive definite [24]. Finally, we assume that $V_{\rm s}(\cdot)$ is continuously differentiable.

Consider the negative feedback interconnection of $\mathcal{G}_{\rm p}$ and $\mathcal{G}_{\rm c}$ given in Figure 1 such that $y = u_{\rm c}$ and $u = -y_{\rm c}$. In this case, the closed-loop system $\mathcal{G}$ is given by

$$\begin{aligned} \dot{x}(t) &= f_{\rm c}(x(t)), \quad x(0) = x_0, \quad x(t) \notin \mathcal{Z}, \quad t \geq 0, \quad (6) \\ \Delta x(t) &= f_{\rm d}(x(t)), \quad x(t) \in \mathcal{Z}, \quad (7) \end{aligned}$$

where $t \geq 0$, $x(t) \triangleq [x_{\rm p}^{\rm T}(t), x_{\rm c}^{\rm T}(t)]^{\rm T}$, $\mathcal{Z} = \{x \in \mathcal{D} : (x_{\rm c}, h_{\rm p}(x_{\rm p})) \in \mathcal{Z}_{\rm c}\}$,

$$f_{\rm c}(x) = \left[\begin{array}{c} f_{\rm p}(x_{\rm p}, -h_{\rm cc}(x_{\rm c}, h_{\rm p}(x_{\rm p}))) \\ f_{\rm cc}(x_{\rm c}, h_{\rm p}(x_{\rm p})) \end{array} \right], \quad (8)$$

$$f_{\rm d}(x) = \left[\begin{array}{c} 0 \\ \eta(h_{\rm p}(x_{\rm p})) - x_{\rm c} \end{array} \right]. \quad (9)$$

Assume that there exists an infinitely differentiable function $V_{\rm c} : \mathcal{D}_{\rm c} \times \mathbb{R}^l \to \overline{\mathbb{R}}_+$ such that $V_{\rm c}(x_{\rm c}, y) \geq 0$, $x_{\rm c} \in \mathcal{D}_{\rm c}$, $y \in \mathbb{R}^l$, and $V_{\rm c}(x_{\rm c}, y) = 0$ if and only if $x_{\rm c} = \eta(y)$ and

$$\begin{aligned} \dot{V}_{\rm c}(x_{\rm c}(t), y(t)) = s_{\rm c}(u_{\rm c}(t), y_{\rm c}(t)), \\ (x_{\rm c}(t), y(t)) \notin \mathcal{Z}, \quad t \geq 0, \quad (10) \end{aligned}$$

where $s_{\rm c} : \mathbb{R}^l \times \mathbb{R}^m \to \mathbb{R}$ is such that $s_{\rm c}(0,0) = 0$ and is locally integrable for all input-output pairs satisfying (3)–(5).

We associate with the plant a positive-definite, continuously differentiable function $V_{\rm p}(x_{\rm p}) \triangleq V_{\rm s}(x_{\rm p})$, which we will refer to as the *plant energy*. Furthermore, we associate with the controller a nonnegative-definite, infinitely differentiable function $V_{\rm c}(x_{\rm c}, y)$ called the controller *emulated energy*. Finally, we associate with the closed-loop system the function

$$V(x) \triangleq V_{\rm p}(x_{\rm p}) + V_{\rm c}(x_{\rm c}, h_{\rm p}(x_{\rm p})), \quad (11)$$

called the *total energy*.

Next, we construct the resetting set for the closed-loop system $\mathcal{G}$ in the following form

$$\begin{aligned} \mathcal{Z} = \{(x_{\rm p}, x_{\rm c}) \in \mathcal{D}_{\rm p} \times \mathcal{D}_{\rm c} : L_{f_{\rm c}} V_{\rm c}(x_{\rm c}, h_{\rm p}(x_{\rm p})) = 0 \quad (12) \\ \text{and } V_{\rm c}(x_{\rm c}, h_{\rm p}(x_{\rm p})) > 0\}, \quad (13) \end{aligned}$$

where $L_{f_{\rm c}} V_{\rm c}(x) \triangleq \frac{\partial V_{\rm c}(x)}{\partial x} f_{\rm c}(x)$ denotes the first-order Lie derivative. The resetting set $\mathcal{Z}$ is thus defined to be the set of all points in the closed-loop state space that correspond to decreasing controller emulated energy. By resetting the controller states, the plant energy can never increase after the first resetting event. Furthermore, if the continuous-time dynamics of the closed-loop system are lossless and the closed-loop system total energy is conserved between resetting events, then a decrease in plant energy is accompanied by a corresponding increase in emulated energy. Hence, this approach allows the plant energy to flow to the controller, where it increases the emulated energy but does not allow the emulated energy to flow back to the plant after the first resetting event. This energy-dissipating hybrid controller effectively enforces a one-way energy transfer between the plant and the controller after the first resetting event. For practical implementation, knowledge of $x_{\rm c}$ and y is sufficient to determine whether or not the closed-loop state vector is in the set $\mathcal{Z}$.

For the next result, recall that the *Lie derivative* of a smooth function $\mathcal{X} : \mathcal{D} \to \mathbb{R}$ along the vector field of the continuous-time dynamics $f_{\rm c}(x)$ is given by $L_{f_{\rm c}} \mathcal{X}(x) \triangleq \frac{\rm d}{{\rm d}t} \mathcal{X}(\psi(t,x))|_{t=0} = \frac{\partial \mathcal{X}(x)}{\partial x} f_{\rm c}(x)$, and the *zeroth* and *higher-order Lie derivatives* are, respectively, defined by $L_{f_{\rm c}}^0 \mathcal{X}(x) \triangleq \mathcal{X}(x)$ and $L_{f_{\rm c}}^k \mathcal{X}(x) \triangleq L_{f_{\rm c}}(L_{f_{\rm c}}^{k-1} \mathcal{X}(x))$, where $k \geq 1$.

Definition 2.1: Let $\mathcal{M} \triangleq \{x \in \mathcal{D} : \mathcal{X}(x) = 0\}$, where $\mathcal{X} : \mathcal{D} \to \mathbb{R}$ is an infinitely differentiable function. A point $x \in \mathcal{M}$ such that $f_{\rm c}(x) \neq 0$ is *k-transversal* to (6) if there exists $k \in \{1, 2, \ldots\}$ such that

$$L_{f_{\rm c}}^r \mathcal{X}(x) = 0, \quad r = 0, \ldots, 2k-2, \quad L_{f_{\rm c}}^{2k-1} \mathcal{X}(x) \neq 0. \quad (14)$$

The next theorem gives sufficient conditions for asymptotic stability of the closed-loop system $\mathcal{G}$ using state-dependent hybrid controllers.

Theorem 2.1 ([12]): Consider the closed-loop hybrid dynamical system $\mathcal{G}$ given by (6) and (7) with the resetting set $\mathcal{Z}$ given by (13). Assume that $\mathcal{D}_{\rm ci} \subset \mathcal{D}$ is a compact positively invariant set with respect to $\mathcal{G}$ such that $0 \in \mathring{\mathcal{D}}_{\rm ci}$, assume that $\mathcal{G}_{\rm p}$ is lossless with respect to the supply rate $s(u,y)$ and with a positive definite, continuously differentiable storage function $V_{\rm p}(x_{\rm p})$, $x_{\rm p} \in \mathcal{D}_{\rm p}$, and assume there exists a smooth (i.e., infinitely differentiable) function $V_{\rm c} : \mathcal{D}_{\rm c} \times \mathbb{R}^l \to \overline{\mathbb{R}}_+$ such that $V_{\rm c}(x_{\rm c}, y) \geq 0$, $x_{\rm c} \in \mathcal{D}_{\rm c}$, $y \in \mathbb{R}^l$, and $V_{\rm c}(x_{\rm c}, y) = 0$ if and only if $x_{\rm c} = \eta(y)$ and (10) holds. Furthermore, assume that every $x_0 \in \overline{\mathcal{Z}}$ is k-transversal to (6) and

$$s(u,y) + s_{\rm c}(u_{\rm c}, y_{\rm c}) = 0, \quad x \notin \mathcal{Z}, \tag{15}$$

where $y = u_{\rm c} = h_{\rm p}(x_{\rm p})$, $u = -y_{\rm c} = -h_{\rm cc}(x_{\rm c}, h_{\rm p}(x_{\rm p}))$, and $\mathcal{Z}$ is given by (13). Then the zero solution $x(t) \equiv 0$ to the closed-loop system $\mathcal{G}$ is asymptotically stable. In addition, the total energy function $V(x)$ of $\mathcal{G}$ given by (11) is strictly decreasing across resetting events. Finally, if $\mathcal{D}_{\rm p} = \mathbb{R}^{n_{\rm p}}$, $\mathcal{D}_{\rm c} = \mathbb{R}^{n_{\rm c}}$, and $V(\cdot)$ is radially unbounded, then the above asymptotic stability results are global.

Remark 2.1: It was shown in [17] that Theorem 2.1 can be generalized to the case where $\mathcal{G}_{\rm p}$ is *dissipative* with respect to the supply rate $s_{\rm p}(u,y)$. In this case, a dissipation rate function does not add any additional complexity to the hybrid stabilization process. See [17] for details.

III. Lagrangian and Hamiltonian Dynamical Systems

Consider the governing equations of motion of an $\hat{n}_{\rm p}$-degree-of-freedom dynamical system given by the *Euler-Lagrange* equation

$$\frac{\rm d}{{\rm d}t}\left[\frac{\partial \mathcal{L}}{\partial \dot{q}}(q(t),\dot{q}(t))\right]^{\rm T} - \left[\frac{\partial \mathcal{L}}{\partial q}(q(t),\dot{q}(t))\right]^{\rm T} = u(t), \quad q(0) = q_0, \quad \dot{q}(0) = \dot{q}_0, \tag{16}$$

where $t \geq 0$, $q \in \mathbb{R}^{\hat{n}_{\rm p}}$ represents the generalized system positions, $\dot{q} \in \mathbb{R}^{\hat{n}_{\rm p}}$ represents the generalized system velocities, $\mathcal{L} : \mathbb{R}^{\hat{n}_{\rm p}} \times \mathbb{R}^{\hat{n}_{\rm p}} \to \mathbb{R}$ denotes the system Lagrangian given by $\mathcal{L}(q,\dot{q}) = T(q,\dot{q}) - U(q)$, where $T : \mathbb{R}^{\hat{n}_{\rm p}} \times \mathbb{R}^{\hat{n}_{\rm p}} \to \mathbb{R}$ is the system kinetic energy and $U : \mathbb{R}^{\hat{n}_{\rm p}} \to \mathbb{R}$ is the system potential energy, and $u \in \mathbb{R}^{\hat{n}_{\rm p}}$ is the vector of generalized control forces acting on the system. Furthermore, let $\mathcal{H} : \mathbb{R}^{\hat{n}_{\rm p}} \times \mathbb{R}^{\hat{n}_{\rm p}} \to \mathbb{R}$ denote the *Legendre transformation* of the Lagrangian function $\mathcal{L}(q,\dot{q})$ with respect to the generalized velocity $\dot{q}$ defined by $\mathcal{H}(q,p) \triangleq \dot{q}^{\rm T}p - \mathcal{L}(q,\dot{q})$, where p denotes the vector of generalized momenta given by $p(q,\dot{q}) = \left[\frac{\partial \mathcal{L}}{\partial \dot{q}}(q,\dot{q})\right]^{\rm T}$, and where the map from the generalized velocities $\dot{q}$ to the generalized momenta p is assumed to be *bijective* (i.e., one-to-one and onto).

Next, we present a hybrid feedback control framework for Euler-Lagrange dynamical systems. Specifically, consider the Lagrangian system (16) with outputs

$$y = \left[\begin{array}{c} h_1(q) \\ h_2(\dot{q}) \end{array}\right] = \left[\begin{array}{c} h_1(q) \\ h_2\left(\frac{\partial \mathcal{H}}{\partial p}(q,p)\right) \end{array}\right], \tag{17}$$

where $h_1 : \mathbb{R}^{\hat{n}_{\rm p}} \to \mathbb{R}^{l_1}$ and $h_2 : \mathbb{R}^{\hat{n}_{\rm p}} \to \mathbb{R}^{l-l_1}$ are continuously differentiable, $h_1(0) = 0$, $h_2(0) = 0$, and $h_1(q) \not\equiv 0$. We assume that the system kinetic energy is such that $T(q,\dot{q}) = \frac{1}{2}\dot{q}^{\rm T}[\frac{\partial T}{\partial \dot{q}}(q,\dot{q})]^{\rm T}$, $T(q,0) = 0$, and $T(q,\dot{q}) > 0$, $\dot{q} \neq 0$, $\dot{q} \in \mathbb{R}^{\hat{n}_{\rm p}}$. We also assume that the system potential energy $U(\cdot)$ is such that $U(0) = 0$ and $U(q) > 0$, $q \neq 0$, $q \in \mathcal{D}_{\rm q} \subseteq \mathbb{R}^{\hat{n}_{\rm p}}$, which implies that $\mathcal{H}(q,p) = T(q,\dot{q}) + U(q) > 0$, $(q,\dot{q}) \neq 0$, $(q,\dot{q}) \in \mathcal{D}_{\rm q} \times \mathbb{R}^{\hat{n}_{\rm p}}$.

Next, consider the energy-based hybrid controller

$$\frac{\rm d}{{\rm d}t}\left[\frac{\partial \mathcal{L}_{\rm c}}{\partial \dot{q}_{\rm c}}(q_{\rm c}(t),\dot{q}_{\rm c}(t),y_q(t))\right]^{\rm T} - \left[\frac{\partial \mathcal{L}_{\rm c}}{\partial q_{\rm c}}(q_{\rm c}(t),\dot{q}_{\rm c}(t),y_q(t))\right]^{\rm T} = 0,$$
$$q_{\rm c}(0) = q_{\rm c0}, \ \dot{q}_{\rm c}(0) = \dot{q}_{\rm c0}, \ (q_{\rm c}(t),\dot{q}_{\rm c}(t),y(t)) \notin \mathcal{Z}_{\rm c}, \tag{18}$$
$$\left[\begin{array}{c} \Delta q_{\rm c}(t) \\ \Delta \dot{q}_{\rm c}(t) \end{array}\right] = \left[\begin{array}{c} \eta(y_q(t)) - q_{\rm c}(t) \\ -\dot{q}_{\rm c}(t) \end{array}\right], \quad (q_{\rm c}(t),\dot{q}_{\rm c}(t),y(t)) \in \mathcal{Z}_{\rm c}, \tag{19}$$
$$u(t) = \left[\frac{\partial \mathcal{L}_{\rm c}}{\partial q}(q_{\rm c}(t),\dot{q}_{\rm c}(t),y_q(t))\right]^{\rm T}, \tag{20}$$

where $t \geq 0$, $q_{\rm c} \in \mathbb{R}^{\hat{n}_{\rm c}}$ represents virtual controller positions, $\dot{q}_{\rm c} \in \mathbb{R}^{\hat{n}_{\rm c}}$ represents virtual controller velocities, $y_q \triangleq h_1(q)$, $\mathcal{L}_{\rm c} : \mathbb{R}^{\hat{n}_{\rm c}} \times \mathbb{R}^{\hat{n}_{\rm c}} \times \mathbb{R}^{l_1} \to \mathbb{R}$ denotes the controller Lagrangian given by $\mathcal{L}_{\rm c}(q_{\rm c},\dot{q}_{\rm c},y_q) \triangleq T_{\rm c}(q_{\rm c},\dot{q}_{\rm c}) - U_{\rm c}(q_{\rm c},y_q)$, where $T_{\rm c} : \mathbb{R}^{\hat{n}_{\rm c}} \times \mathbb{R}^{\hat{n}_{\rm c}} \to \mathbb{R}$ is the controller kinetic energy and $U_{\rm c} : \mathbb{R}^{\hat{n}_{\rm c}} \times \mathbb{R}^{l_1} \to \mathbb{R}$ is the controller potential energy, $\eta(\cdot)$ is a continuously differentiable function such that $\eta(0) = 0$, $\mathcal{Z}_{\rm c} \subset \mathbb{R}^{\hat{n}_{\rm c}} \times \mathbb{R}^{\hat{n}_{\rm c}} \times \mathbb{R}^l$ is the resetting set, $\Delta q_{\rm c}(t) \triangleq q_{\rm c}(t^+) - q_{\rm c}(t)$, and $\Delta \dot{q}_{\rm c}(t) \triangleq \dot{q}_{\rm c}(t^+) - \dot{q}_{\rm c}(t)$. We assume that the controller kinetic energy $T_{\rm c}(q_{\rm c},\dot{q}_{\rm c})$ is such that $T_{\rm c}(q_{\rm c},\dot{q}_{\rm c}) = \frac{1}{2}\dot{q}_{\rm c}^{\rm T}[\frac{\partial T_{\rm c}}{\partial \dot{q}_{\rm c}}(q_{\rm c},\dot{q}_{\rm c})]^{\rm T}$, with $T_{\rm c}(q_{\rm c},0) = 0$ and $T_{\rm c}(q_{\rm c},\dot{q}_{\rm c}) > 0$, $\dot{q}_{\rm c} \neq 0$, $\dot{q}_{\rm c} \in \mathbb{R}^{\hat{n}_{\rm c}}$. Furthermore, we assume that $U_{\rm c}(\eta(y_q),y_q) = 0$ and $U_{\rm c}(q_{\rm c},y_q) > 0$ for $q_{\rm c} \neq \eta(y_q)$, $q_{\rm c} \in \mathcal{D}_{\rm q_c} \subseteq \mathbb{R}^{\hat{n}_{\rm c}}$.

As in Section II, note that $V_{\rm p}(q,\dot{q}) \triangleq T(q,\dot{q}) + U(q)$ is the plant energy and $V_{\rm c}(q_{\rm c},\dot{q}_{\rm c},y_q) \triangleq T_{\rm c}(q_{\rm c},\dot{q}_{\rm c}) + U_{\rm c}(q_{\rm c},y_q)$ is the controller emulated energy. Finally,

$$V(q,\dot{q},q_{\rm c},\dot{q}_{\rm c}) \triangleq V_{\rm p}(q,\dot{q}) + V_{\rm c}(q_{\rm c},\dot{q}_{\rm c},y_q) \tag{21}$$

is the total energy of the closed-loop system. For the closed-loop system, we define our resetting set as $\mathcal{Z} \triangleq \{(q,\dot{q},q_{\rm c},\dot{q}_{\rm c}) : (q_{\rm c},\dot{q}_{\rm c},y) \in \mathcal{Z}_{\rm c}\}$. It was shown in [12] that along the closed-loop system trajectories

$$\frac{\rm d}{{\rm d}t}V(q(t),\dot{q}(t),q_{\rm c}(t),\dot{q}_{\rm c}(t)) = 0, \quad (q(t),\dot{q}(t),q_{\rm c}(t),\dot{q}_{\rm c}(t)) \notin \mathcal{Z}, \quad t_k < t \leq t_{k+1}, \tag{22}$$
$$\Delta V(q(t_k),\dot{q}(t_k),q_{\rm c}(t_k),\dot{q}_{\rm c}(t_k)) = -V_{\rm c}(q_{\rm c}(t_k),\dot{q}_{\rm c}(t_k),y_q(t_k)), < 0, \quad (q(t_k),\dot{q}(t_k),q_{\rm c}(t_k),\dot{q}_{\rm c}(t_k)) \in \mathcal{Z}, \quad k \in \overline{\mathbb{Z}}_+, \tag{23}$$

which implies that the total energy of the closed-loop system between resetting events is conserved and that the resetting law (19) ensures the total energy decrease across resetting events by an amount equal to the accumulated emulated energy.

Here, we consider an energy-dissipating state-dependent resetting controller that affects a one-way energy transfer between the plant and the controller. Specifically, consider

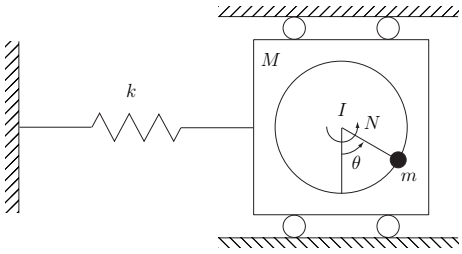

Fig. 2. Rotational/translational proof-mass actuator.

Description	Parameter	Value	Units
Cart mass	M	1.7428	kg
Eccentric mass	m	0.2739	kg
Arm eccentricity	e	0.0537	m
Arm inertia	I	0.000884	$\mathrm{kg\,m^2}$
Spring stiffness	k	339.4	N/m
Controller parameter	m_{c}	0.0004	—
Controller parameter	k_{c}	0.2317	—

TABLE I

PROBLEM DATA FOR THE RTAC SYSTEM.

the closed-loop system (16), (17)–(20), where $\mathcal{Z}$ is defined by

$$\mathcal{Z} \triangleq \left\{ (q, \dot{q}, q_{\mathrm{c}}, \dot{q}_{\mathrm{c}}) : \frac{\mathrm{d}}{\mathrm{d}t} V_{\mathrm{c}}(q_{\mathrm{c}}, \dot{q}_{\mathrm{c}}, y_q) = 0 \right. \\ \left. \text{and } V_{\mathrm{c}}(q_{\mathrm{c}}, \dot{q}_{\mathrm{c}}, y_q) > 0 \right\}. \quad (24)$$

Once again, for practical implementation, knowledge of q_{c}, $\dot{q}_{\mathrm{c}}$, and y_q is sufficient to determine whether or not the closed-loop state vector is in the set $\mathcal{Z}$.

The next theorem gives sufficient conditions for stabilization of Euler-Lagrange dynamical systems using state-dependent hybrid controllers. For this result define the closed-loop system states $x \triangleq [q^{\mathrm{T}}, \dot{q}^{\mathrm{T}}, q_{\mathrm{c}}^{\mathrm{T}}, \dot{q}_{\mathrm{c}}^{\mathrm{T}}]^{\mathrm{T}}$.

Theorem 3.1 ([12]): Consider the closed-loop dynamical system $\mathcal{G}$ given by (16), (17)–(20), with the resetting set $\mathcal{Z}$ given by (24). Assume that $\mathcal{D}_{\mathrm{ci}} \subset \mathcal{D}_{\mathrm{q}} \times \mathbb{R}^{\hat{n}_{\mathrm{p}}} \times \mathcal{D}_{\mathrm{q_c}} \times \mathbb{R}^{\hat{n}_{\mathrm{c}}}$ is a compact positively invariant set with respect to $\mathcal{G}$ such that $0 \in \overset{\circ}{\mathcal{D}}_{\mathrm{ci}}$. Furthermore, assume that the k-transversality condition (14) holds with $\mathcal{X}(x) = \frac{\mathrm{d}}{\mathrm{d}t} V_{\mathrm{c}}(q_{\mathrm{c}}, \dot{q}_{\mathrm{c}}, y_q)$. Then the zero solution $x(t) \equiv 0$ to $\mathcal{G}$ is asymptotically stable. Finally, if $\mathcal{D}_{\mathrm{q}} = \mathbb{R}^{\hat{n}_{\mathrm{p}}}$, $\mathcal{D}_{\mathrm{q_c}} = \mathbb{R}^{\hat{n}_{\mathrm{c}}}$, and the total energy function $V(x)$ is radially unbounded, then the above asymptotic stability results are global.

IV. RTAC System

In this section, we describe the rotational/translational proof-mass actuator (RTAC) nonlinear system studied in [19]. The system (see Figure 2) involves an eccentric rotational inertia, which acts as a proof-mass actuator mounted on a translational oscillator cart. Rotational motion of the proof-mass is nonlinearly coupled with translational motion of the cart which provides the mechanism for control action. The oscillator cart of mass M is connected to a fixed support via a linear spring of stiffness k. The cart is constrained to one-dimensional motion and the rotational proof-mass actuator consists of a mass m and mass moment of inertia I located a distance e from the center of mass of the cart. In Figure 2, N denotes the control torque applied to the proof mass.

Letting q, $\dot{q}$, θ, and $\dot{\theta}$ denote the translational position and velocity of the cart and the angular position and velocity of the rotational proof mass, respectively, and using the energy function

$$V_{\mathrm{s}}(q, \dot{q}, \theta, \dot{\theta}) = \frac{1}{2}[kq^2 + (M+m)\dot{q}^2 + (I + me^2)\dot{\theta}^2 \\ + 2me\dot{q}\dot{\theta}\cos\theta] + mge(1 - \cos\theta), \quad (25)$$

the nonlinear dynamic equations of motion are given by

$$(M+m)\ddot{q} + kq = -me(\ddot{\theta}\cos\theta - \dot{\theta}^2 \sin\theta), \quad (26)$$

$$(I + me^2)\ddot{\theta} = -me\ddot{q}\cos\theta - mge\sin\theta + N, \quad (27)$$

with problem data given in Table I, control input $u = N$, and output $y = \theta$.

To design a state-dependent hybrid controller for (26) and (26), let $n_{\mathrm{c}} = 1$, $V_{\mathrm{c}}(q_{\mathrm{c}}, \dot{q}_{\mathrm{c}}, \theta) = \frac{1}{2}m_{\mathrm{c}}\dot{q}_{\mathrm{c}}^2 + \frac{1}{2}k_{\mathrm{c}}(q_{\mathrm{c}} - \theta)^2$, $\mathcal{L}_{\mathrm{c}}(q_{\mathrm{c}}, \dot{q}_{\mathrm{c}}, \theta) = \frac{1}{2}m_{\mathrm{c}}\dot{q}_{\mathrm{c}}^2 - \frac{1}{2}k_{\mathrm{c}}(q_{\mathrm{c}} - \theta)^2$, $y_q = \theta$, and $\eta(y_q) = y_q$, where $m_{\mathrm{c}} > 0$ and $k_{\mathrm{c}} > 0$. Then the state-dependent hybrid controller has the form

$$m_{\mathrm{c}}\ddot{q}_{\mathrm{c}} + k_{\mathrm{c}}(q_{\mathrm{c}} - \theta) = 0, \quad (q_{\mathrm{c}}, \dot{q}_{\mathrm{c}}, \theta, \dot{\theta}) \notin \mathcal{Z}, \quad (28)$$

$$\begin{bmatrix} \Delta q_{\mathrm{c}} \\ \Delta \dot{q}_{\mathrm{c}} \end{bmatrix} = \begin{bmatrix} \theta - q_{\mathrm{c}} \\ -\dot{q}_{\mathrm{c}} \end{bmatrix}, \quad (q_{\mathrm{c}}, \dot{q}_{\mathrm{c}}, \theta, \dot{\theta}) \in \mathcal{Z}, \quad (29)$$

$$u = k_{\mathrm{c}}(q_{\mathrm{c}} - \theta), \quad (30)$$

with the resetting set (24) taking the form

$$\mathcal{Z} = \left\{ (q_{\mathrm{c}}, \dot{q}_{\mathrm{c}}, \theta, \dot{\theta}) \in \mathbb{R}^4 : k_{\mathrm{c}}\dot{\theta}(q_{\mathrm{c}} - \theta) = 0 \right. \\ \left. \text{and } \begin{bmatrix} \theta - q_{\mathrm{c}} \\ -\dot{q}_{\mathrm{c}} \end{bmatrix} \neq 0 \right\}. \quad (31)$$

It was shown in [17] that the closed-loop system (26), (27), and (28)–(31) satisfies k-transversality condition given in Definition 2.1, and hence, by Theorem 3.1, is globally asymptotically stable. In the next section, we implement the developed energy-based hybrid control framework to the RTAC testbed and present the experimental results.

V. Hardware Description and Experimental Results

The experimental testbed constructed to implement the energy-based hybrid control system is shown in Figure 3. It consists of an aluminum base with two rails that air bushings float on providing translational motion for the cart with very low friction. A rotary actuator with an eccentric arm and a mass are fixed to the cart providing the control torque. The actuation is provided by a DC motor driven by a linear motor controller, and the measurements of the eccentric arm angle and cart position are performed with a quadrature encoder and laser displacement sensor, respectively. The controller is implemented with the MathWorks MATLAB®, Simulink®, and xPC Target software using National Instruments PCI cards for I/O. The hardware used for the testbed is listed in Table II. Next, we provide a more detailed description of the experimental testbed.

Translational motion of the cart is provided by four air bushings mounted into aluminum blocks. These blocks are mounted to an aluminum plate to form the platform of the cart. This platform is also constructed to deliver air to the bushings through internal passageways to eliminate excessive air fittings. The air bushings float on two stainless steel precision shafts of 0.5 in in diameter that are affixed to the aluminum base. This configuration leads to a very low friction coefficient resulting in a damping ratio of 0.23% with

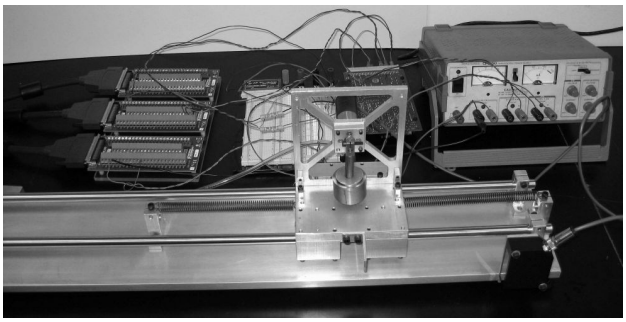

Fig. 3. RTAC testbed.

Description	Manufacturer	Model
Air Bushing	New Way bearings	S301201
Laser sensor	Micro-Epsilon	ILD1300-200
DC motor	MicroMo	3863H012C
Shaft Encoder	MicroMo	HEDM5500J12
Motor Controller	Advanced Motion Controls	12A8
DAQ board	National Instruments	NI6024E
Encoder/Timer	National Instruments	NI 6601

TABLE II

MODEL AND MANUFACTURER INFORMATION OF HARDWARE USED.

the pendulum fixed. A support is attached to the platform to facilitate mounting of the rotational actuator and proof-mass. The support is designed in such a manner that it could be mounted either vertically or horizontally. This enables the experiment to be carried out with and without gravitational effect on the proof-mass. Two pretensioned extension springs are attached on opposite sides of the cart and are connected to fixed supports on the base. The springs are easy to remove so that springs with different stiffness can be used. The effective spring stiffness constant for the testbed was measured to be 339.4 N/m and the spring is shown to be linear throughout the useable range. The natural frequency of the platform without any motion from the proof-mass was experimentally determined to be 2.15 Hz, and the carts travel is limited to ± 3 in resulting from the maximum permissible extension of the springs.

The control torque for the system is provided by means of a proof-mass attached to an actuator by an eccentric arm. The arm is constructed in such a way that various proof-masses may be used, and the actuator is a 12 volt DC motor. The motor generates a continuous torque of 0.110 N·m with a stall torque of 1.200 N·m, and has a thermally limited continuous current of 7.6 A. Driving the motor is a PWM servo amplifier which can supply a peak current of 12 A and a continuous current of 6 A. The unit is operated in current mode producing a current which is proportional to the input voltage. The motor controller has a built-in current limiter to protect the motor from high torque commands.

Measurement of the systems states was accomplished with a quadrature encoder and a laser displacement sensor. The quadrature encoder was used to measure the angular position and velocity of the proof-mass. The encoder is attached to the back of the motor and has a 1024 line per revolution resolution. This gives an angular resolution of 0.09° when used in quadrature mode. Position and velocity of the translational mass is measured with a laser sensor that uses optical triangulation to measure displacement. The sensor measures position with an accuracy of 200 μm at a rate of 500 Hz. A laser sensor was selected over other linear measurement sensors since it does not influence the motion of the carriage.

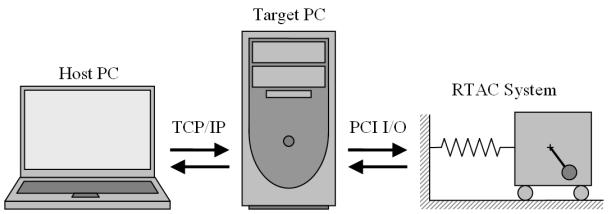

Fig. 4. Diagram of real-time target implementation.

To implement the energy-based hybrid control system in real time the MathWorks MATLAB®, Simulink®, and xPC Target software was used. The diagram in Figure 4 illustrates the hardware layout. The control law is created in Simulink®, compiled into C code, and then downloaded onto the target PC. The target PC runs a real time operating system that executes the Simulink® block diagram. The Input/Output for the target PC consists of National Instruments PCI-6024E and PCI-6601 PCI cards. The PCI-6024E is used to acquire the distance measured by the laser sensor, and to send a voltage to the motor controller to generate the required control torque, while the PCI-6601 card is used to read the encoder to obtain the angle and direction of rotation of the proof-mass.

Next, we show experimental results obtained from implementing the energy-based control framework presented in Sections II and III on the RTAC testbed. The system parameters are shown in Table I with initial conditions $q(0) = -0.051$ m, $\dot{q}(0) = 0$, $\theta(0) = 0$, $\dot{\theta}(0) = 0$, $q_c(0) = 0$, and $\dot{q}_c(0) = 0$. Figure 5 shows cart position and pendulum angle versus time. Figure 6 shows time history of the controller states. Note that the controller states are discontinuous according to (29). The control torque versus time is shown in Figure 7. It is discontinuous at the resetting times as follows from (30). Figure 8 shows the plant, controller emulated, and total energies of the RTAC system. Although the sum of the plant energy and controller emulated energy is supposed to remain constant between resettings as shown in (22), in the experimental setup the small increases in total energy are result of numerical errors due to measurement noise.

REFERENCES

[1] A. van der Schaft, "Stabilization of Hamiltonian systems," *Nonlinear Analysis: Theory, Methods, and Applications*, vol. 10, pp. 1021–1035, 1986.

[2] R. Ortega and M. W. Spong, "Adaptive motion control of rigid robots: A tutorial," *Automatica*, vol. 25, pp. 877–888, 1989.

[3] H. Nijmeijer and A. J. van der Schaft, *Nonlinear Dynamical Control Systems*. New York, NY: Springer, 1990.

[4] R. Ortega, A. Loria, R. Kelly, and L. Praly, "On output feedback global stabilization of Euler-Lagrange systems," *Int. J. Contr.*, vol. 5, pp. 313–324, 1995.

[5] S. Shishkin, R. Ortega, D. Hill, and A. Loria, "On output feedback stabilization of Euler-Lagrange systems with nondissipative forces," *Sys. Contr. Lett.*, vol. 27, pp. 315–324, 1996.

[6] R. Ortega, A. Loria, P. J. Nicklasson, and H. Sira-Ramírez, *Passivity-Based Control of Euler-Lagrange Systems*. London, UK: Springer-Verlag, 1998.

[7] R. Ortega, A. van der Schaft, B. Maschke, and G. Escobar, "Energy-shaping of port-controlled Hamiltonian systems," in *Proc. Conf. Dec. Contr.*, Phoenix, AZ, December 1999, pp. 1646–1651.

[8] R. Ortega, A. van der Schaft, and B. Maschke, "Stabilization of port-controlled Hamiltonian systems via energy balancing," in *Stability and Stabilization of Nonlinear Systems*, D. Aeyels, F. Lamnabhi-Lagarrigue, and A. van der Schaft, Eds. London, UK: Springer-Verlag, 1999.

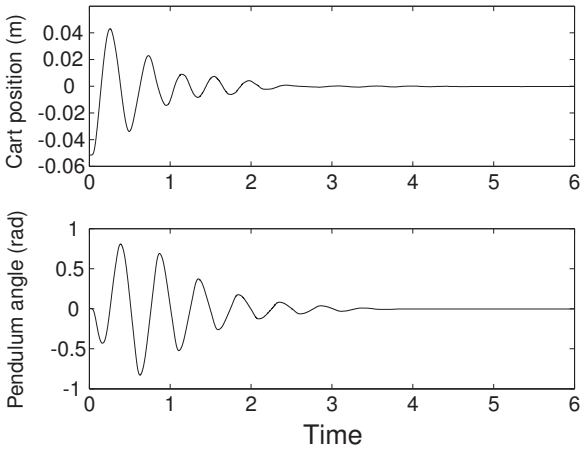

Fig. 5. Cart position and pendulum angle versus time.

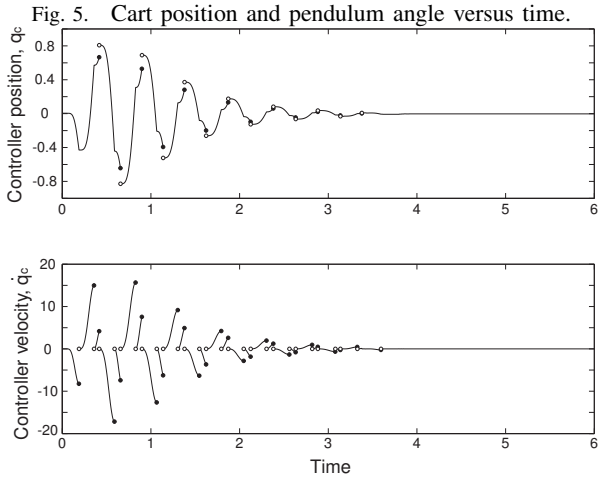

Fig. 6. Controller position and velocity variables versus time.

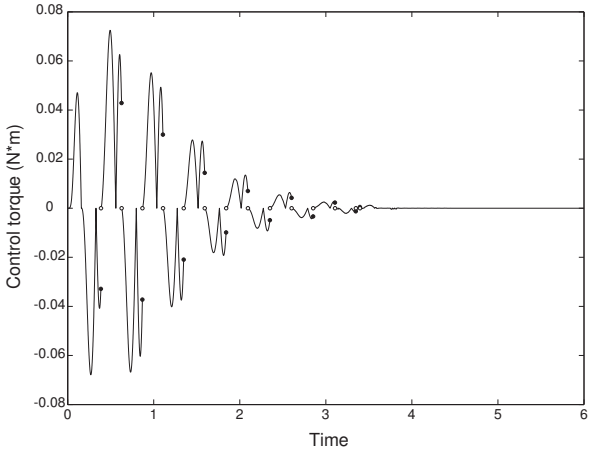

Fig. 7. Control torque versus time.

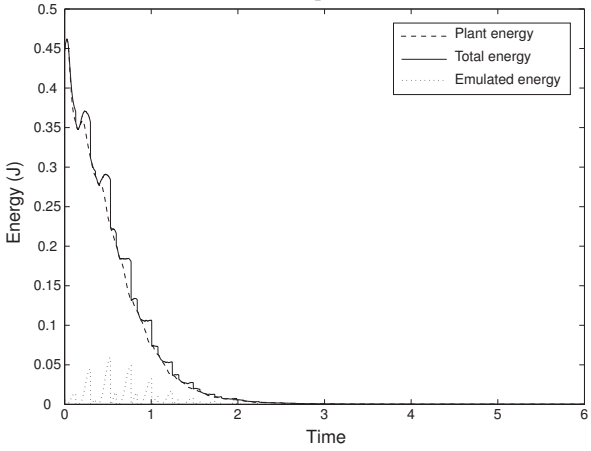

Fig. 8. Plant, controller emulated, and total energies versus time.

[9] R. Ortega, A. van der Schaft, B. Maschke, and G. Escobar, "Interconnection and damping assignment passivity-based control of port-controlled Hamiltonian systems," *Automatica*, vol. 38, pp. 585–596, 2002.

[10] A. van der Schaft, *L_2-Gain and Passivity Techniques in Nonlinear Control*. London, UK: Springer-Verlag, 2000.

[11] S. Prajna, A. J. van der Schaft, and G. Meinsma, "An LMI approach to stabilization of linear port-controlled Hamiltonian systems," *Sys. Contr. Lett.*, vol. 45, pp. 371–385, 2002.

[12] W. M. Haddad, V. Chellaboina, Q. Hui, and S. G. Nersesov, "Energy- and entropy-based stabilization for lossless dynamical systems via hybrid controllers," *IEEE Trans. Autom. Contr.*, vol. 52, no. 9, pp. 1604–1614, 2007.

[13] Y. Kishimoto and D. S. Bernstein, "Thermodynamic modeling of interconnected systems I: Conservative coupling," *J. Sound Vibr.*, vol. 182, pp. 23–58, 1995.

[14] A. F. Filippov, *Differential Equations with Discontinuous Right-Hand Sides*. Mathematics and its Applications (Soviet Series), Dordrecht: Kluwer Academic Publishers, 1988.

[15] V. Lakshmikantham, D. D. Bainov, and P. S. Simeonov, *Theory of Impulsive Differential Equations*. Singapore: World Scientific, 1989.

[16] D. D. Bainov and P. S. Simeonov, *Systems with Impulse Effect: Stability, Theory and Applications*. England: Ellis Horwood Limited, 1989.

[17] W. M. Haddad, V. Chellaboina, and S. G. Nersesov, *Impulsive and Hybrid Dynamical Systems. Stability, Dissipativity, and Control*. Princeton, NJ: Princeton University Press, 2006.

[18] R. T. Bupp, D. S. Bernstein, V. Chellaboina, and W. M. Haddad, "Resetting virtual absorbers for vibration control," *J. Vibr. Contr.*, vol. 6, pp. 61–83, 2000.

[19] R. T. Bupp, D. S. Bernstein, and V. T. Coppola, "A benchmark problem for nonlinear control design," *Int. J. Robust and Nonlinear Control*, vol. 8, pp. 307–310, 1998.

[20] M. Antonio and W. Yu, "Nonlinear benchmark system identification with partial states measurement," in *Proc. IEEE Conf. Dec. Contr.*, Phoenix, AZ, 1999, pp. 1077–1082.

[21] R. T. Bupp, D. S. Bernstein, and V. T. Coppola, "Experimental implementation of integrator backstepping and passive nonlinear controllers on the RTAC testbed," *Int. J. Robust and Nonlinear Control*, vol. 8, pp. 435–457, 1998.

[22] I. Kolmanovsky and H. McClamroch, "Hybrid feedback stabilization of rotational translational actuator (RTAC) system," *Int. J. Robust and Nonlinear Control*, vol. 8, pp. 367–375, 1998.

[23] J. C. Willems, "Dissipative dynamical systems. Part I: General theory," *Arch. Rational Mech. Anal.*, vol. 45, pp. 321–351, 1972.

[24] D. J. Hill and P. J. Moylan, "Dissipative dynamical systems: Basic input-output and state properties," *J. Franklin Insitute*, vol. 309, pp. 327–357, 1980.